



# High-precision measurements of seawater Pb isotope compositions by double spike thermal ionization mass spectrometry



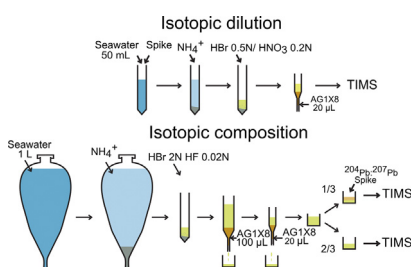
Maxence Paul\*, Luke Bridgestock, Mark Rehkämper, Tina van DeFliedert, Dominik Weiss

Department of Earth Science & Engineering, Imperial College London, London SW7 2AZ, UK

## HIGHLIGHTS

- Precise and accurate determination of seawater Pb isotope compositions.
- Uncertainties (2sd) for  $^{206}\text{Pb}/^{204}\text{Pb}$ ,  $^{207}\text{Pb}/^{204}\text{Pb}$ ,  $^{208}\text{Pb}/^{204}\text{Pb}$  are better than  $\pm 3\%$ .
- Analysis of a GEOTRACES depth profile from the South Atlantic Ocean.
- Pb isotopic compositions reflect the different water masses that were sampled.
- The  $^{207}\text{Pb}/^{206}\text{Pb}$  and  $^{206}\text{Pb}/^{204}\text{Pb}$  ratios display a correlation.

## GRAPHICAL ABSTRACT



## ARTICLE INFO

### Article history:

Received 24 September 2014  
 Received in revised form 4 December 2014  
 Accepted 5 December 2014  
 Available online 10 December 2014

### Keywords:

Seawater  
 Lead isotope  
 Double spike  
 Thermal ionization mass spectrometry  
 GEOTRACES  
 Inter-calibration

## ABSTRACT

A new method for the determination of seawater Pb isotope compositions and concentrations was developed, which combines and optimizes previously published protocols for the separation and isotopic analysis of this element. For isotopic analysis, the procedure involves initial separation of Pb from 1 to 2 L of seawater by coprecipitation with Mg hydroxide and further purification by a two stage anion exchange procedure. The Pb isotope measurements are subsequently carried out by thermal ionization mass spectrometry using a  $^{207}\text{Pb}$ - $^{204}\text{Pb}$  double spike for correction of instrumental mass fractionation. These methods are associated with a total procedural Pb blank of  $28 \pm 21$  pg (1sd) and typical Pb recoveries of 40–60%. The Pb concentrations are determined by isotope dilution (ID) on 50 mL of seawater, using a simplified version of above methods. Analyses of multiple aliquots of six seawater samples yield a reproducibility of about  $\pm 1$  to  $\pm 10\%$  (1sd) for Pb concentrations of between 7 and 50 pmol/kg, where precision was primarily limited by the uncertainty of the blank correction ( $12 \pm 4$  pg; 1sd). For the Pb isotope analyses, typical reproducibilities ( $\pm 2$ sd) of 700–1500 ppm and 1000–2000 ppm were achieved for  $^{207}\text{Pb}/^{206}\text{Pb}$ ,  $^{208}\text{Pb}/^{206}\text{Pb}$  and  $^{206}\text{Pb}/^{204}\text{Pb}$ ,  $^{207}\text{Pb}/^{204}\text{Pb}$ ,  $^{208}\text{Pb}/^{204}\text{Pb}$ , respectively. These results are superior to literature data that were obtained using plasma source mass spectrometry and they are at least a factor of five more precise for ratios involving the minor  $^{204}\text{Pb}$  isotope. Both Pb concentration and isotope data, furthermore, show good agreement with published results for two seawater intercomparison samples of the GEOTRACES program. Finally, the new methods were applied to a seawater depth profile from the eastern South Atlantic. Both Pb contents and isotope compositions display a smooth evolution with depth, and no obvious outliers. Compared to previous Pb isotope data for seawater, the  $^{206}\text{Pb}/^{204}\text{Pb}$  ratios are well correlated with  $^{207}\text{Pb}/^{206}\text{Pb}$ , underlining the significant improvement achieved in the measurement of the minor  $^{204}\text{Pb}$  isotope.

© 2014 The Authors. Published by Elsevier B.V. This is an open access article under the CC BY license (<http://creativecommons.org/licenses/by/3.0/>).

\* Corresponding author. Tel.: +44 20 7594 6391; fax: +44 20 7589 5111.  
 E-mail address: [maxence.paul@gmail.com](mailto:maxence.paul@gmail.com) (M. Paul).

## 1. Introduction

Investigations that map the distribution of trace metals and their isotopes in seawater and which study their relationship to and potential impacts on global biogeochemical cycles in the oceans are an overarching goal of modern marine geochemistry and a key objective of the international GEOTRACES program [1]. The global scale impact of human activities on natural Pb budgets was established more than 40 years ago by Chow and co-workers [2–5] and massive inputs of anthropogenic Pb into the oceans were soon thereafter identified by Patterson and co-workers [6–8], based on the first accurate and precise Pb concentration measurements for seawater. Studies of the anthropogenic impact on marine Pb budgets were further advanced with the first successful Pb isotope analyses of seawater [6,9–13]. Whilst these early measurements were all carried out by TIMS (thermal ionization mass spectrometry), the majority of seawater Pb analyses since the 1990s have been conducted using various types of ICP-MS instrumentation. At present, the most precise Pb isotope analyses of seawater apply either single collector high resolution or multiple collector ICP-MS (HR-ICP-MS and MC-ICP-MS, respectively), most commonly following low-blank pre-concentration of the element by co-precipitation with  $\text{Mg}(\text{OH})_2$  [14,15].

These methodological advances are a consequence of the particular importance of seawater Pb isotope data to studies of environmental pollution and marine geochemistry. For example, analyses of corals yielded a seawater Pb isotope record for the North Atlantic over the last 220 years [12,15,16], which revealed significant isotopic variability through time, in accord with known changes in the extent and type of anthropogenic emissions. Similarly, Pb isotope data for the modern ocean are used to infer the distribution of Pb from different anthropogenic and natural sources in surface seawater [9,13,17,18] and to determine the lateral mixing and advection of subsurface water masses [19–23]. Shen and Boyle [12], furthermore, highlighted that temporal changes in the Pb content and isotope composition of different water masses can be applied to trace ventilation times.

In this paper, we present a new method for the accurate and precise determination of seawater Pb concentrations and isotope compositions. The methodology involves pre-concentration of Pb by  $\text{Mg}(\text{OH})_2$  co-precipitation [24] followed by ion exchange chromatography [25,26], and subsequent isotopic analyses by TIMS using a  $^{204}\text{Pb}$ – $^{207}\text{Pb}$  double spike to achieve precise control of instrumental mass fractionation [27,28]. The technique is validated by analyses of both in-house and international seawater reference materials and its utility demonstrated by data obtained for a GEOTRACES seawater depth profile from the South Atlantic Ocean.

A number of previous investigations [28–34] have shown that the application of Pb double or triple spikes enables Pb isotope measurements that are significantly more precise and accurate than conventional TIMS or MC-ICP-MS techniques and less susceptible to the analytical artifacts, which can be generated by instrumental mass bias effects. Our study is the first to apply the double spike methodology to seawater Pb isotope analyses. Using these techniques, we are not only able to analyze the commonly measured ratios  $^{207}\text{Pb}/^{206}\text{Pb}$ ,  $^{208}\text{Pb}/^{206}\text{Pb}$  to high precision but  $^{206}\text{Pb}/^{204}\text{Pb}$ ,  $^{207}\text{Pb}/^{204}\text{Pb}$  and  $^{208}\text{Pb}/^{204}\text{Pb}$  can also be determined to an uncertainty of better than about  $\pm 3\%$ . Only very scarce seawater data are available for the latter ratios due to the analytical challenges but measurements of non-radiogenic  $^{204}\text{Pb}$  are deemed to be important to fully exploit the potential of the Pb isotope system.

## 2. Experimental

### 2.1. Samples

A gravimetric solution of the well-characterized NIST standard reference material SRM 981 Pb was employed for calibration of the Pb double spike and to evaluate the precision of the mass spectrometric methods. Four filtered seawater samples that were available in large quantities were utilized as in house reference materials to further assess reproducibility. These encompass a surface water sample (Atlantic – S) and three subsurface water samples, Atlantic – D1, Atlantic – D2 (both from 2000 m depth), and Weddell (400 m depth). These samples were not specifically collected for Pb isotope analyses, and potential contamination during sampling and initial handling hence renders them unsuitable for evaluation of accuracy or an assessment of water mass properties.

To enable a comparison of our results with literature data for assessment of accuracy, we analyzed the international seawater reference samples GSI and GDI. These were collected at water depths of 7 m and 2000 m, respectively, at the Bermuda Atlantic Ocean Time Series station (BATS) during the 2008 GEOTRACES intercalibration cruise on the R/V Knorr (KN193-6). The collection and handling of these samples employed materials and procedures that were specifically designed for the intercalibration of contamination-prone trace metals and isotopes [35].

The seawater for a Pb isotope and concentration depth profile was collected in the South Atlantic Ocean off the African coast at 36.46°S, 13.39°E in October 2010 during the eastern part of the GEOTRACES GA10 transect along 40°S on the R.R.S. Discovery (D357; 18 October–22 November 2010) [1]. This depth profile from station 3 encompasses 12 samples that cover the entire 4500 m of the water column at the sampling location. Station 3 serves as a ‘cross over station’, which means that it was sampled by three separate GEOTRACES cruises (UK GEOTRACES cruise D357 – this study; UK GEOTRACES cruise JC068 in 2011/2012; MD166 BONUS – GoodHope Cruise in 2008, Boye et al. [36]), thereby enabling a comparison of results for samples from a single location but that were collected at different times and analyzed using different methodologies. The samples from cruise D357 analyzed here were obtained with a titanium rosette deployed from plasma rope and equipped with trace metal clean sample bottles and supplemented by underway surface water sampling (2–3 m depth) using a towed ‘fish’ (Wyatt et al. [37]). All bottle handling was conducted in a clean container and each sample was transferred into two pre-cleaned 1 L LPDE bottles without filtration or acidification. About one year after collection and two weeks prior to analysis, the samples were acidified to pH 2 with 6 M HCl.

### 2.2. Reagents

Water with a resistivity of  $>18.2 \text{ M}\Omega \text{ cm}$  from a Milli-Q water system was used throughout for reagent preparation and cleaning of labware. Purified concentrated HF ( $\sim 28 \text{ M}$ ) and HBr ( $\sim 8.5 \text{ M}$ ) were purchased from VWR as Optima (distilled) grade acids whilst concentrated (14.5 M)  $\text{HNO}_3$  and 6 M HCl were prepared in-house by subboiling distillation of reagent grade acids in quartz stills. The Pb blanks of these acids were checked regularly and found to be consistently less than 2 pg/mL. The dilute mineral acids that were employed for the separation chemistry were freshly prepared for each batch of samples.

A purified aqueous solution of  $\text{NH}_3$  was used to affect precipitation of  $\text{Mg}(\text{OH})_2$  from seawater and prepared by cold vapor phase equilibration of reagent grade 28% (w/w) aqueous  $\text{NH}_3$  with Milli-Q water in a Savillex Teflon elbow. Approximately 2 volumes of 28% aqueous  $\text{NH}_3$  were employed for each

volume of Milli-Q water, and these were equilibrated for about two weeks to obtain purified aqueous  $\text{NH}_3$  (aq- $\text{NH}_3$ ) at a concentration of about 9 M. During this period, the Teflon elbow was stored double bagged in plastic, to limit contamination and loss of gaseous  $\text{NH}_3$ . The aq- $\text{NH}_3$  was collected from the still just prior to use and each batch of three samples, plus a full procedural blank, was treated with the same solution. The Pb blank of the aqueous ammonia was stable at less than 0.3 pg/mL during the course of the study.

### 2.3. Preparation and calibration of $^{207}\text{Pb}$ – $^{204}\text{Pb}$ double spike

Highly enriched (>99%) metallic  $^{204}\text{Pb}$  and  $^{207}\text{Pb}$  in wire form were purchased from Isoflex (USA). The wires were separately dissolved in 7.5 M  $\text{HNO}_3$  and diluted with water to obtain solutions in 2 M  $\text{HNO}_3$ . A dilute double spike solution was then prepared with a total Pb concentration of  $\sim 10$  ng/mL and an optimal molar ratio of  $^{207}\text{Pb}/^{204}\text{Pb} \approx 1$ , based on the error propagation modeling of Galer [28] and Rudge [38].

Spike calibration was performed using a gravimetric solution of NIST SRM 981 Pb. In a first step, the concentration of the double spike was determined by two reverse isotope dilution runs that were carried out with a Nu Plasma HR MC-ICP-MS, using external normalization to added Tl for mass bias control [24,39,40]. Initially, a preliminary concentration was obtained, based on an approximate spike isotope compositions, which was calculated from the mixing proportions of the  $^{204}\text{Pb}$  and  $^{207}\text{Pb}$  solutions, and the respective isotope compositions, as supplied by Isoflex.

The isotope composition of the double spike (Table 1) was then calibrated by analyses of different gravimetrically prepared double spike – NIST SRM 981 mixtures using TIMS [38,41]. The instrumental mass fractionation correction [24,39,40], the spike-standard mixing line, and the double spike composition were calculated by over-determining the system of equations (number of double spike – NIST SRM 981 mixtures >2) and solving in the least-square sense, as described by Rudge et al. [38]. Finally, the calibrated double spike isotope composition was applied to the data from the initial reverse isotope dilution runs, to accurately define the double spike concentration.

### 2.4. Sample preparation for determination of Pb isotope compositions

#### 2.4.1. Lead pre-concentration by co-precipitation with magnesium hydroxide

A number of previous studies have shown that co-precipitation of Pb with  $\text{Mg}(\text{OH})_2$  is an effective, low-blank method for pre-concentration of Pb from seawater [14,42] and this technique is retained in our procedure. Initial tests showed that Pb is efficiently and reproducibly extracted from seawater at yields  $\geq 80\%$  by precipitation with  $\text{Mg}(\text{OH})_2$  at  $\text{pH} \approx 10$ . The yields were, furthermore, not correlated with the exact pH value that was adjusted or the amount of  $\text{Mg}(\text{OH})_2$  precipitated. The  $\text{Mg}(\text{OH})_2$  precipitate, however, was also found to scavenge a significant amount of sea salt, but the latter could be removed without noticeable reduction of the Pb yield by rinsing the precipitate with water.

In order to obtain sufficient Pb for precise analyses, even for Pb depleted seawater from the deep ocean, samples of up to about 2 L were processed. The seawater was transferred to 1 L pre-cleaned Teflon separating funnels, to aid the collection of the Mg hydroxide precipitate. Precipitation of  $\text{Mg}(\text{OH})_2$  was affected by introduction of the purified aq- $\text{NH}_3$  until a final pH value of about 10 was obtained. As each seawater sample had been acidified to a slightly different extent, and because the precipitate forms only gradually, the applied volume of aq- $\text{NH}_3$  was optimized for each sample by slowly adding successive portions of the reagent to the separating funnel. This was achieved by an initial addition of 2–4 mL aq- $\text{NH}_3$ , whereupon the samples were stirred vigorously and then left to stand for at least 3 h to allow the  $\text{Mg}(\text{OH})_2$  precipitate to form. If precipitation had not occurred after this time, an additional volume of 0.5 mL of aq- $\text{NH}_3$  was added every 2–3 h until formation of precipitate was observed.

Once about 5 mL of  $\text{Mg}(\text{OH})_2$  slurry had formed, the precipitate was drained through the bottom of the separating funnel, collected in a 15 mL Teflon centrifuge tube, centrifuged at 1700 rpm for about 10 min and the remaining solution poured off. This step was repeated several times until all precipitate was recovered from the funnel. The solids were then washed with 5 mL  $\text{H}_2\text{O}$ , centrifuged again and finally dissolved directly in the tubes by addition of 5 mL of a 2 M  $\text{HBr}$ –0.01 M  $\text{HF}$  acid mixture. To aid dissolution, the centrifuge tubes were shaken whereupon the formation of many small bubbles within the solutions was observed for seawater

**Table 1**

Lead isotope data of this study and reference values for NIST SRM 981 Pb. Also shown is the isotope composition of the Pb double spike used in this study.

Sample	Pb used (ng) <sup>a</sup>	<i>n</i> <sup>b</sup>	$^{206}\text{Pb}/^{204}\text{Pb} \pm 2\text{sd}^c$	$^{207}\text{Pb}/^{204}\text{Pb} \pm 2\text{sd}^c$	$^{208}\text{Pb}/^{204}\text{Pb} \pm 2\text{sd}^c$	$^{207}\text{Pb}/^{206}\text{Pb} \pm 2\text{sd}^c$	$^{208}\text{Pb}/^{206}\text{Pb} \pm 2\text{sd}^c$
This study							
SRM 981 Pb	2	42	16.943 ± 16	15.496 ± 15	36.716 ± 38	0.91460 ± 18	2.16710 ± 61
±2sd relative (ppm)			920	970	1050	200	280
±2se of typical (ppm) <sup>d</sup>			~500	~500	~550	~60	~80
SRM 981 Pb	10	25	16.9419 ± 31	15.4968 ± 38	36.7224 ± 91	0.91470 ± 11	2.16755 ± 20
±2sd relative (ppm) <sup>e</sup>			180	240	250	120	90
±2se of typical run			~90	~100	~100	~40	~60
SRM 981 Reference values <sup>e</sup>							
Galer and Abouchami (TIMS) [57]	~10		16.9405 ± 15	15.4963 ± 16	36.7219 ± 44	0.91475 ± 4	2.16771 ± 10
Thirlwall (TIMS) [31]	~20		16.9409 ± 22	15.4956 ± 26	36.7228 ± 80	0.91469 ± 7	2.16770 ± 21
Todt et al. (TIMS) [58]	80		16.9356 ± 23	15.4891 ± 30	36.7006 ± 113	0.91459 ± 13	2.16701 ± 43
Thirlwall (MC-ICP-MS) [32]			16.9417 ± 29	15.4996 ± 31	36.724 ± 9	0.91488 ± 8	2.16770 ± 24
Baker et al. (MC-ICP-MS) [29]	~50		16.9416 ± 13	15.5000 ± 13	36.7262 ± 31	0.91491 ± 4	2.16781 ± 12
$^{207}\text{Pb}$ – $^{204}\text{Pb}$ double spike <sup>f</sup>			0.00240	1.03181	0.00820	431.03	3.4267

<sup>a</sup> Mass of Pb loaded on filament and/or used for a single analysis.

<sup>b</sup> *n* = number of analyses.

<sup>c</sup> 2sd = 2 × standard deviation calculated from *n* separate runs; denotes long-term “external” reproducibility.

<sup>d</sup> 2se = 2 × standard error of the mean; denotes within-run (“internal”) precision of the data, based on individual results for measurement cycles.

<sup>e</sup> All reference values were obtained using either double or triple spike techniques for correction of instrumental mass fractionation.

<sup>f</sup> Isotope composition of the Pb double spike used in the current study.

samples that had not been filtered following collection. Bubble formation is hence presumably related to the presence of residual organic compounds. It is important to remove the bubbles at this stage because they can otherwise lead to the formation of larger bubbles within the resin bed during the subsequent column chemistry, effectively blocking the flow. For removal of the bubbles, the centrifuge tubes were left to stand overnight, sealed and then gently heated on a hotplate for 10 min at 50 °C. After cooling, bubbles should no longer be visible in the solutions, otherwise the heating was repeated.

#### 2.4.2. Lead purification by anion exchange chromatography

The anion exchange purification procedure for Pb (Table 2) is based on previously published methods that apply strongly basic AG1X8 resin and dilute HBr–HNO<sub>3</sub> mixtures for elution, with modifications as detailed below.

Previous work [14,43,44] has shown that silica is trapped by the Mg(OH)<sub>2</sub> precipitate, which is used for the separation of Pb from seawater. Relatively high Si concentrations of about 10–150 μmol/kg are, furthermore, found in seawater samples from depths >1000 m [45,46]. During method development we found that such concentrations suffice to form precipitates of silica on top of the resin column, when HF is not present in sample solutions. Hence, the 1st stage column chemistry of our final method (Table 2) applies a 2 M HBr–0.01 M HF mixture for sample loading, whereby the small concentration of HF present enhances silica solubility to prevent precipitation of silicic acid. The same acid mixture is subsequently also used to completely flush silica from the resin, prior to elution of other matrix elements (Table 2). In 2 M HBr, Pb has a distribution coefficient K<sub>D</sub> of about 200 toward the AG1X8 anion exchange resin that was used [25,47,48]. Elution experiments confirmed that, whilst the Pb K<sub>D</sub> value is reduced when HF is present, the use of trace HF in the elution scheme (Table 2) does not prevent retention of Pb on the resin bed during sample loading and matrix elution.

Following elution of Pb from the 1st stage columns, the samples were dried and further purified by a second column chemistry step, which is needed to eliminate remaining traces of Mg [49] and improve the ionization of Pb during the TIMS analyses. To this end, the dried samples were redissolved in 0.2 M HBr–0.5 M HNO<sub>3</sub> and processed using established HBr–HNO<sub>3</sub> procedures on small 20 μL resin columns (Table 2), which help to minimize the procedural blank.

#### 2.5. TIMS analyses of Pb isotope compositions

The accurate determination of Pb isotope compositions with precise correction of instrumental mass discrimination requires

two separate mass spectrometric runs – one of the pure sample and a second analysis of a double spike – sample mixture. To this end, the purified Pb was divided into two aliquots and the double spike was admixed to one, prior to the TIMS measurements. The addition of the double spike after, rather than before, the chemical separation of Pb has a number of advantages. Conveniently, each sample needs to be processed through the (time-consuming) pre-concentration and purification steps only once, rather than twice. Furthermore, the impact of contamination from reagents and handling is minimized and uncertainties arising from different blanks impacting on the spiked and unspiked analyses are reduced.

In detail, our procedure involves splitting the Pb solutions from the 2nd stage column chemistry into a larger and a smaller aliquot. The larger aliquot comprising 2/3 of the sample remained unspiked, whilst Pb double spike was added to the remaining aliquot with 1/3 of the solution. The double spike addition was thereby carried out to obtain a molar ratio of natural (N) to spike-derived Pb (S) that approximates the optimum S/N ≈ 1.226 [38]. This is equivalent to a molar proportion of spike, S/(S+N), of 55.1%, corresponding to <sup>206</sup>Pb/<sup>204</sup>Pb ≈ 0.411 (assuming a natural seawater <sup>206</sup>Pb/<sup>204</sup>Pb = 18.4). The amount of natural Pb present was thereby estimated from the Pb concentration measurements that were carried out first for all samples, and assuming a Pb recovery of 60% from the chemical separation (see below).

Following aliquoting and spiking, the Pb solutions were evaporated to dryness and redissolved in 1 μL 2 M HNO<sub>3</sub>. The samples were loaded on a single, previously outgassed zone refined Re filament (99.999%; H. Cross, USA), dried at 0.4 A, 0.5 μL of silica–gel activator was then added and also dried at 0.4 A. The sample–activator mixture was finally heated at 2 A for ~1 s to evaporate phosphoric acid and fuse the silica gel.

Gerstenberger and Hasse [50] prepared a highly successful activator for Pb isotope analyses by TIMS but this applies silica particles which are no longer commercially available. Hence, a new SiO<sub>2</sub>–H<sub>3</sub>PO<sub>4</sub> activator mixture was made up for the current study. This mixture was prepared from SiO<sub>2</sub> nanoparticles (20–60 nm; Iolitec Inc.) and Merck Ultrapur phosphoric acid, whereby a SiO<sub>2</sub>/H<sub>3</sub>PO<sub>4</sub> weight ratio of 0.43% was applied with respect to the addition of the silica to dilute 0.16 M H<sub>3</sub>PO<sub>4</sub>. The amount of activator used for analysis was calibrated to optimize ionization yields, based on tests that were carried out with 2 ng NIST 981 Pb. These tests revealed that use of 0.5 μL activator solution was preferable to loading with 1 μL of activator – whilst the latter yielded more stable Pb ion beams the former produced ion beam intensities that were typically about 2–3 times higher.

The Pb isotope measurements were carried out on a TRITON TIMS instrument operating in static mode and using Faraday cups

**Table 2**  
Column chemistry procedure for the separation of Pb from seawater for isotope compositions (IC) and isotope dilution (ID) concentration measurements by TIMS

	Pb IC chemistry 1st stage	Pb IC chemistry 2nd stage	Pb ID chemistry
Resin <sup>a</sup>	100 μL AG1X8, 100–200 mesh	20 μL AG1X8, 100–200 mesh	20 μL AG1X8, 100–200 mesh
Clean resin	3 × 3 mL 0.1 M HNO <sub>3</sub>	3 × 1 mL 0.1 M HNO <sub>3</sub>	3 × 1 mL 0.1 M HNO <sub>3</sub>
Equilibrate resin	2 × 0.1 mL 2 M HBr–0.01 M HF	2 × 0.1 mL 0.2 M HBr–0.5 M HNO <sub>3</sub>	2 × 0.1 mL 0.5 M HBr–0.2 M HNO <sub>3</sub>
Load sample	~5 mL in 2 M HBr–0.01 M HF	~1 mL in 0.2 M HBr–0.5 M HNO <sub>3</sub>	2 mL 0.5 M HBr–0.2 M HNO <sub>3</sub>
Elute matrix	2 × 0.1 mL 2 M HBr–0.01 M HF	2 × 0.3 mL 0.2 M HBr–0.5 M HNO <sub>3</sub>	2 × 0.3 mL 0.5 M HBr–0.2 M HNO <sub>3</sub>
Elute Pb	2 × 0.5 mL 0.2 M HBr–0.01 M HNO <sub>3</sub> 0.2 mL 0.03 M HBr–0.5 M HNO <sub>3</sub>	1 mL 0.03 M HBr–0.5 M HNO <sub>3</sub>	1 mL 0.03 M HBr–0.5 M HNO <sub>3</sub>

<sup>a</sup> The resin is used in columns prepared from shrink-fit Teflon tubing. The columns have a reservoir volume of ~3 mL and a resin column with an internal diameter of ~3 mm.

fitted with  $10^{11} \Omega$  resistors. Prior to each measurement session, a gain calibration was carried out for all amplifiers. For analysis, the filaments were heated to a target temperature of about  $1300^\circ\text{C}$  within 30 min, and isotopic data were then collected in 15 blocks of 15 cycles with an integration time of 8.3 s. Half-mass baseline measurements (30 cycles  $\times$  1.05 s integrations following 5 s idle time) and an automatic peak centering routine (followed by 3 s idle time) were carried out prior to each block. Loads of 2 ng NIST 981 Pb provided stable and very reproducible ion beam intensities of 200–300 mV  $^{208}\text{Pb}$ . For the seawater samples, the ion beam intensities were more variable and generally lower, whereby 2 ng Pb generally yielded  $^{208}\text{Pb}$  ion beams of about 100–200 mV.

The measured isotopic data for the spiked and unspiked sample aliquots were processed using an iterative solver that employs published methods [38] and which was implemented as a macro within a Microsoft Excel spreadsheet. The method uses the exponential law to obtain mass bias corrected Pb isotope data and is employed on a cycle-by-cycle basis to provide an accurate assessment of the final propagated data uncertainties.

Following Doucelance and Manhès [51], the TIMS source was baked for 3 h after the introduction of a new sample turret. This technique was observed to substantially reduce the formation of hydrocarbon species that can form inferring molecular ions during the Pb isotope runs [31]. The baking also significantly improved the vacuum within the ion source (to about  $3.5$  to  $6 \times 10^{-8}$  mbar, without use of a liquid  $\text{N}_2$  cold trap) and enhanced Pb ion beam stability, thereby permitting analyses without interblock re-heating. The latter improvement is presumably due to the efficient drying of the silica gel, which is achieved during heating in vacuum condition.

Barium- $\text{PO}_x$  ions were mainly observed at temperatures, which are slightly higher compared to those employed for optimal Pb ionization [31]. The formation of such ions, and hence the presence of Ba in samples, is best avoided because they produce minor molecular interferences on  $^{204}\text{Pb}$  (from  $^{138}\text{Ba}^{31}\text{P}^{17}\text{O}^{18}\text{O}^{+}$ ,  $^{137}\text{Ba}^{31}\text{P}^{18}\text{O}_2^+$ ) and, even more problematic, hinder the ionization of Pb whereby rapidly decaying Pb ion beams are observed. The presence of  $\text{BaPO}_x$  ions was routinely monitored during the analyses at mass 201, which corresponds primarily to  $^{138}\text{Ba}^{31}\text{P}^{16}\text{O}_2^+$ . The measured ion beam intensities at mass 201 were observed to rise during Pb sample runs but only to maximum values of 1–3 mV. At this level, the  $\text{BaPO}_2$  interference contributes less than 15 ppm to the  $^{204}\text{Pb}$  ion beam, such that a correction was deemed unnecessary.

### 2.6. Determination of Pb concentrations

Lead concentrations were determined by isotope dilution (ID), and using a chemical separation method similar to that employed for the isotope ratio measurements but optimized for the processing of smaller seawater samples. In detail, 50 mL of seawater were weighed into clean polyethylene centrifuge tubes. Following addition of the Pb double spike, the mixtures were left to stand for at least 10 days to ensure full spike–sample equilibration. The amount of Pb spike added was based on an initial ‘guess’ of or any information available for the Pb concentration of the samples, to achieve an optimal  $S/N \approx 2.61$  (equivalent to  $^{206}\text{Pb}/^{204}\text{Pb} \approx 0.188$ ) for minimal error propagation during ID data reduction.

Co-precipitation of Pb with  $\text{Mg}(\text{OH})_2$  was affected by adding 150  $\mu\text{L}$  of purified aq- $\text{NH}_3$ . Following separation of the precipitate by centrifugation and dissolution in a dilute  $\text{HNO}_3$ – $\text{HBr}$  mixture, Pb was further purified using a single stage anion exchange chemistry. This employed small resin columns of only 20  $\mu\text{L}$  to minimize the procedural blank (Table 2). The anion exchange chemistry was slightly modified in comparison to the 2nd stage

chemistry for Pb isotopes through use of a 0.5 M  $\text{HBr}$ –0.2 M  $\text{HNO}_3$  acid mixture for sample loading and matrix elution, because this was observed to facilitate the dissolution of the  $\text{Mg}(\text{OH})_2$  precipitate whilst ensuring quantitative retention of Pb on the small resin columns.

The ID TIMS analyses for Pb used the same techniques that were applied for the isotopic measurements but with shorter runs comprising 5 blocks of 15 cycles. During filament loading of some samples for the ID TIMS analyses, the presence of impurities, in the form of salts and possibly also organic compounds, was detected. When present, such impurities were associated with poor Pb ion beam intensities during the TIMS runs and in some extreme cases the analyses were even abandoned. Such contamination may also produce interfering molecular ions that could generate inaccurate ID results. Subsequent test showed that the impurities can be reduced to negligible levels, by allowing the resin bed to drain and dry completely (for about 10 min) after each step of the column chemistry procedure for Pb separation (Table 2) and, in particular, prior to the elution of Pb.

## 3. Results and discussion

### 3.1. Blanks

The total blank for the Pb isotope measurements was determined by carrying out the complete analytical procedure without an initial seawater sample being present. Over a 24-month period, the mean procedural blank was  $28 \pm 21$  pg (1sd,  $n=25$ ; ignoring two abnormally high blanks of  $\sim 100$  pg encountered during a single two-week period). The individual contributions to this total from (i) filament loading and (ii) reagents were also determined and found to be  $1.9 \pm 0.5$  pg for the former,  $5.0 \pm 1.4$  pg for the mineral acids used, and  $2.5 \pm 0.2$  pg for the aq- $\text{NH}_3$  solutions. The contribution of the anion exchange resin and column chemistry (without reagents) to the total blank could hence be quantified as  $17 \pm 8$  pg, by subtracting the reagent component from separately measured column chemistry blanks. The sum of the individual blank contributions is, therefore,  $27 \pm 10$  pg, in accord with the full procedural blanks values determined during the study. Ignoring the individual contributions (and chemistry yields), a Pb blank of 10–50 pg contributes about 0.05–2.5% to the indigenous Pb budget of samples that were analyzed for isotopic compositions, assuming samples volumes and Pb concentrations of 1–2 L and 10–50 pmol/kg, respectively. The Pb isotope composition of the blank was also measured on several occasions with rather variable results, due to the low ion beam intensities and/or actual differences in blank compositions (e.g.,  $^{206}\text{Pb}/^{204}\text{Pb} = 18.34 \pm 0.62$ ,  $^{207}\text{Pb}/^{206}\text{Pb} = 1.196 \pm 0.028$ ,  $^{208}\text{Pb}/^{206}\text{Pb} = 2.422 \pm 0.021$ ; 2se,  $n=10$ ). Blank corrections were not applied to the isotopic data because such corrections did not improve the reproducibility of results from replicate sample analyses (see discussion below).

The total procedural blank for the Pb ID concentration measurements was determined using 100  $\mu\text{L}$  seawater samples, as only negligible amounts of Pb ( $\sim 0.2$  to 1 pg) are present in such small volumes. These measurements revealed a relatively stable total Pb blank of  $11.7 \pm 4.3$  pg (1sd,  $n=36$ ), which is equivalent to about 1–15% to the indigenous Pb in ID sample aliquots, assuming Pb abundances of 10–50 pmol/kg (for simplicity, this ignores variable chemistry yields and individual blank contributions). Blank corrections were applied to all measured Pb concentrations based on the mean blank value. The uncertainties of the Pb concentration data propagate both the (within-run) precision of the isotopic analyses and the uncertainty of the blank correction.

### 3.2. Chemical separation of Pb

Stable isotope fractionation of Pb during anion exchange chromatography with HCl was recently documented and shown to vary systematically with Pb recovery [29,52]. Such fractionation can have a detrimental impact on the accuracy of subsequent Pb isotope measurements and may also occur during Pb purification with other anion exchange elution protocols. As part of this study, it was, therefore, investigated whether incomplete recovery of Pb from the anion exchange chemistry applied here (Table 2) also has a systematic impact on the measured Pb isotope compositions. To this end, multiple 10 ng aliquots of NIST SRM 981 Pb were processed through the complete 2-stage column separation procedure and the purified Pb fractions were then analyzed using standard methods. The data (Fig. 1) illustrate that the column chemistry routinely affords Pb yields of about 50–70%. Such recoveries are in accord with the total Pb yields of about 30–60% that were determined for multiple analyses of five different seawater samples (Tables 3 and 4). Assuming that the Mg(OH)<sub>2</sub> co-precipitation achieves a recovery of ≥80% for seawater Pb (see above), the Pb yield of the column chemistry is constrained to be about 40–75%.

In a previous investigation, Reuer et al. [15] reported essentially complete recovery of seawater Pb pre-concentrated by Mg(OH)<sub>2</sub> co-precipitation, during purification on AG1X8 resin (as in this study) but using HBr and HCl for elution [49]. Test conducted during the course of the present study showed, however, that the method of Reuer et al. [15] was associated with Pb recoveries similar to those reported here, when the procedure was modified to include additional use of HF to prevent precipitation of silicic acid during sample loading (Table 2). The use of dilute HF thus appears to be associated with either incomplete Pb retention on or elution from the anion exchange resin, regardless of the exact nature of the mineral acids, which are applied in the procedure. Ultimately, the current HBr-HNO<sub>3</sub> method (Table 2) was preferred to the elution method of Reuer et al. [15], because the former applies only dilute mineral acids (which helps to minimize the blank) and routinely produced cleaner Pb separates for subsequent isotopic analyses.

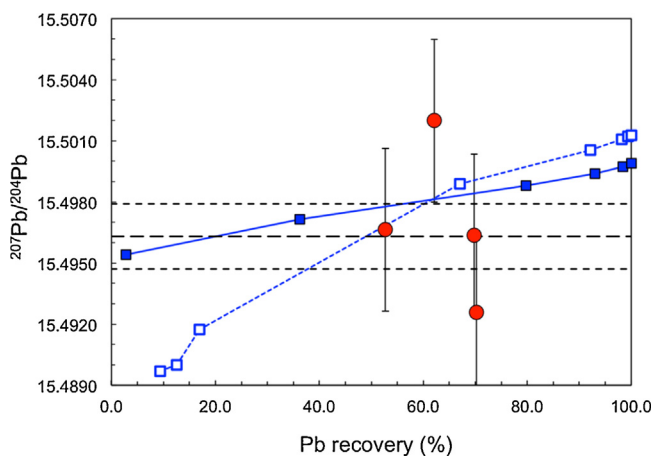


**Fig. 1.** The recovery of Pb and <sup>207</sup>Pb/<sup>204</sup>Pb ratios obtained for 10 ng aliquots of NIST SRM 981 Pb that were processed through the 2-stage column chemistry (Table 2) are shown as full red circles with error bars that denote a ±2sd uncertainty of about 240 ppm (Table 3). Shown for comparison are literature data for cumulative recovery and isotope composition of SRM 981 Pb that was collected in successive fractions from anion-exchange resin which was eluted with HCl: full blue squares and solid line—elution with 6M HCl; open blue squares with hashed line—elution with 2M and 8M HCl (Baker [29]). The dashed black lines indicate the <sup>207</sup>Pb/<sup>204</sup>Pb reference value determined for SRM 981 Pb (15.4963 ± 16; Table 1). (For interpretation of the references to color in this figure legend, the reader is referred to the web version of this article.)

**Table 3**  
Lead concentration and isotope composition data for the four in-house seawater reference materials and other key information relating to samples.

Sample	n- ID <sup>a</sup>	[Pb] ± 1sd pmol/kg <sup>b</sup>	±1sd (%)	n- IC <sup>c</sup>	<sup>205</sup> Pb/ <sup>204</sup> Pb ±2sd <sup>d</sup>	<sup>207</sup> Pb/ <sup>204</sup> Pb ±2sd <sup>d</sup>	<sup>208</sup> Pb/ <sup>204</sup> Pb ±2sd <sup>d</sup>	<sup>207</sup> Pb/ <sup>206</sup> Pb ±2sd <sup>d</sup>	<sup>208</sup> Pb/ <sup>206</sup> Pb ±2sd <sup>d</sup>	Sample size L <sup>e</sup>	Total Pb ng <sup>f</sup>	Meas. Pb (mean) ng <sup>g</sup>	Pb yield (%) <sup>h</sup>
Atlantic - S ±2sd relative (ppm) <sup>d</sup> ±2se typical run (ppm) <sup>i</sup>	6	24.7 ± 1.0	4.0	5	18.429 ± 12 630 ~300	15.639 ± 9 560 ~300	38.307 ± 25 650 ~300	0.84862 ± 98 1150 ~40	2.0787 ± 25 1220 ~50	~2	~11	3–6 (~4)	30–60
Atlantic - D1 ±2sd relative (ppm) <sup>d</sup> ±2se typical run (ppm) <sup>i</sup>	11	45.3 ± 0.5	1.1	7	18.499 ± 30 1610 ~350	15.625 ± 20 1280 ~350	38.287 ± 58 1520 ~350	0.84464 ± 50 590 ~100	2.0697 ± 12 580 ~50	1–2	10–20	3–10 (6)	30–50
Atlantic - D2 ±2sd relative (ppm) <sup>d</sup> ±2se typical run (ppm) <sup>i</sup>	2	47.4 ± 1.2	0.8	7	18.481 ± 30 1730 ~650	15.625 ± 22 1500 ~650	38.272 ± 59 1650 ~700	0.84540 ± 59 760 ~80	2.0707 ± 10 550 ~90	~2	~20	2–15 (7)	10–70
Weddell ±2sd relative (ppm) <sup>d</sup> ±2se typical run (ppm) <sup>i</sup>	8	7.6 ± 1.0	12.3	7	18.397 ± 48 2600 ~600	15.628 ± 20 1300 ~600	38.293 ± 70 1830 ~600	0.84945 ± 147 1730 ~60	2.0814 ± 20 980 ~90	~2	~3.8	~2.0	50–60

<sup>a</sup> Number of individual sample aliquots analyzed for Pb concentrations.

<sup>b</sup> Pb concentrations are corrected for a mean total blank of 11.7 ± 4.3 pg. The uncertainties of the concentration data propagate both the (within-run) precision of the isotopic analyses and the uncertainty of the blank correction (see text).

<sup>c</sup> Number of individual sample aliquots analyzed for Pb isotope compositions.

<sup>d</sup> 2sd = 2 × standard deviation calculated from results of n separate runs; denotes long-term “external” reproducibility.

<sup>e</sup> Volume of individual aliquots used for Pb isotope analyses.

<sup>f</sup> Original mass of Pb in sample aliquots used for Pb isotope analyses.

<sup>g</sup> Mass of Pb in individual aliquots used for isotopic analyses, following chemical separation; a mean value is given in parentheses.

<sup>h</sup> Pb recovery for the chemical separation process.

<sup>i</sup> 2se = 2 × standard error of the mean; denotes within-run (“internal”) precision of a run, based on individual results for measurement cycles.

**Table 4**  
Lead concentration (ID) and isotope composition (IC) data for the GEOTRACES intercalibration samples GSI and GDI and reference values from the literature.

Sample	<i>n</i> -ID <sup>a</sup>	[Pb] ± 1sd pmol/kg <sup>b</sup>	<i>n</i> -IC <sup>c</sup>	<sup>206</sup> Pb/ <sup>204</sup> Pb ± 2sd <sup>d</sup>	<sup>207</sup> Pb/ <sup>204</sup> Pb ± 2sd <sup>d</sup>	<sup>208</sup> Pb/ <sup>204</sup> Pb ± 2sd <sup>d</sup>	<sup>207</sup> Pb/ <sup>206</sup> Pb ± 2sd <sup>d</sup>	<sup>208</sup> Pb/ <sup>206</sup> Pb ± 2sd <sup>d</sup>	Sample size L <sup>e</sup>	Total Pb ng <sup>f</sup>	Pb yield (%) <sup>g</sup>
<b>GSI</b>											
This study	6	27.9 ± 1.2	3	18.359 ± 26	15.635 ± 7	38.246 ± 30	0.85162 ± 93	2.0833 ± 16	~2	~10	45–60
±2sd relative (ppm) <sup>d</sup>				1430	480	790	1100	750			
±2se typical run (ppm) <sup>i</sup>				~160	~170	~180	~30	~40			
Ref. – MIT			5	18.41 ± 11	15.67 ± 9	38.33 ± 23	0.85143 ± 39	2.0821 ± 15	0.25 to –0.5	1.5–3	
±2sd relative (ppm) <sup>d</sup>				5870	5790	6020	460	700			
Ref. – UCSC			2 <sup>h</sup>	18.46 ± 0	15.68 ± 1	38.36 ± 7	0.84929 ± 50	2.0780 ± 40	~0.5	~3	
Ref. – Consensus		29.5 ± 2.1									
<b>GDI</b>											
This study	5	45.7 ± 2.6	2	18.475 ± 41	15.624 ± 10	38.276 ± 60	0.84568 ± 134	2.0718 ± 14	~2	~17	50–55
±2sd relative (ppm) <sup>d</sup>				2240	650	1570	1590	670			
±2se typical run (ppm) <sup>i</sup>				~190	~200	~210	~30	~60			
Ref. – MIT			4	18.74 ± 17	15.83 ± 12	38.79 ± 31	0.84493 ± 214	2.0696 ± 50	0.25 to –0.5	2.5–5	
±2sd relative (ppm) <sup>d</sup>				9320	7330	8000	2530	2410			
Ref. – UCSC			4	18.54 ± 3	15.69 ± 2	38.43 ± 10	0.84640 ± 42	2.0729 ± 27	~0.5	2.5–5	
Ref. – Consensus		42.2 ± 1.3									

The Pb isotope reference data (Ref.) are from the labs of Ed Boyle at the Massachusetts Institute of Technology (MIT) and Russ Flegel at the University of California Santa Cruz (UCSC) [35]. Results in italics were calculated from data given in the literature. The ‘Consensus’ Pb concentrations are from [53].

<sup>a</sup> Number of individual sample aliquots analyzed for Pb concentrations.

<sup>b</sup> Pb concentrations are corrected for a mean total blank of 11.7 ± 4.3 pg. The uncertainties of the concentration data propagate both the (within-run) precision of the isotopic analyses and the uncertainty of the blank correction (see text).

<sup>c</sup> Number of individual sample aliquots analyzed for Pb isotope compositions.

<sup>d</sup> 2sd = 2 × standard deviation calculated from results of *n* separate runs; denotes long-term “external” reproducibility.

<sup>e</sup> Volume of individual aliquots used for Pb isotope analyses.

<sup>f</sup> Original mass of Pb in sample aliquots used for Pb isotope analyses.

<sup>g</sup> Pb recovery for the chemical separation process.

<sup>i</sup> 2se = 2 × standard error of the mean; denotes within-run (“internal”) precision of a run, based on individual results for measurement cycles.

<sup>h</sup> Duplicate analyses of Pb separated from a single seawater sample.

Importantly, the isotope data of Fig. 1 demonstrate that incomplete recovery of Pb from the column separation is not associated with significant shifts in isotopic composition. These results do not, however, rule out small, but barely resolvable, enrichments of heavier Pb isotopes following chemical purification. This follows from the observations of previous studies, which detected only minor Pb isotope fractionations, comparable to or smaller than the reproducibility of our results, as a result of incomplete elution of the element from anion exchange columns (Fig. 1).

### 3.3. Analyses of NIST SRM 981 Pb

Multiple measurements of 2 ng ( $n = 42$ ) and 10 ng ( $n = 25$ ) loads of NIST SRM 981 Pb were carried out for a basic validation for our double spike techniques of Pb isotope analysis. Notably, the mean isotopic data acquired for both the 2 ng and 10 ng runs are in excellent agreement with recent reference values that were acquired using various Pb double or triple spikes in conjunction with analyses by either TIMS or MC-ICP-MS (Table 1).

The 2sd between-run ('external') precision of the 10 ng data is  $\sim 100$  ppm for  $^{207}\text{Pb}/^{206}\text{Pb}$ ,  $^{208}\text{Pb}/^{206}\text{Pb}$  and  $\sim 250$  ppm for  $^{20x}\text{Pb}/^{204}\text{Pb}$  (where  $x = ^{206}\text{Pb}$ ,  $^{207}\text{Pb}$ ,  $^{208}\text{Pb}$  hereafter). This is similar to or only slightly worse than the reproducibility achieved by other workers with TIMS or MC-ICP-MS for comparable or somewhat larger Pb samples (10–80 ng; Table 1). Our data for the 2 ng loads, a sample size that is more relevant for seawater analyses (Table 3), is less precise than the 10 ng results, with a reproducibility ( $\pm 2\text{sd}$  external) of  $\sim 250$  ppm for  $^{207}\text{Pb}/^{206}\text{Pb}$ ,  $^{208}\text{Pb}/^{206}\text{Pb}$  and  $\sim 1000$  ppm for  $^{20x}\text{Pb}/^{204}\text{Pb}$  (Table 3). The significantly larger uncertainty of the  $^{20x}\text{Pb}/^{204}\text{Pb}$  data presumably reflects that the 2 ng Pb analyses were hampered by the measurement of  $^{204}\text{Pb}$  at low ion beam intensities (about 5–20 mV) using a Faraday cup and standard  $10^{11} \Omega$  amplifiers. The within-run ('internal') precision (quantified by 2se; standard error of the mean) of both the 2 and 10 ng Pb measurements are about a factor of 2–3 better compared to the between-run uncertainties for all Pb isotope ratios (Table 1).

### 3.4. Analyses of in-house seawater reference samples

Multiple Pb concentration and isotope ratio analyses were carried out on four different in-house seawater reference samples (Table 3). These were available in sufficient quantity such that 5–7 repeat isotopic analyses could be carried out to rigorously investigate the reproducibility of the methods.

For the Pb contents, the precision (expressed as  $\pm 1\text{sd}$ , as is common for concentration data) varies between less than  $\pm 1\%$  to about  $\pm 12\%$  (Table 3). Notably, the reproducibility is worse for samples with low Pb contents. As similar samples sizes (of only  $\sim 50$  mL) were employed for these measurements, the higher uncertainties for the Pb-depleted samples are most likely related to inaccuracies of the Pb blank correction, possibly due to spurious high blanks.

The isotopic results for the in-house seawater reference samples (Table 3) were acquired on individual aliquots of 1–2 L, from which about 2–10 ng of Pb were separated. The data display a  $\pm 2\text{sd}$  reproducibility of  $\sim 500$ – $1500$  ppm for  $^{207}\text{Pb}/^{206}\text{Pb}$ ,  $^{208}\text{Pb}/^{206}\text{Pb}$  and  $\sim 500$ – $2000$  ppm for  $^{20x}\text{Pb}/^{204}\text{Pb}$  (Table 3). Clearly, this is inferior to the 2sd precision that was obtained for the comparable 2 ng and 10 ng loads of pure NIST SRM 981 Pb (Table 1). At the same time, the internal (within-run)  $\pm 2\text{se}$  precision of the seawater measurements is similar to the NIST SRM 981 results, with uncertainties of  $\sim 40$ – $100$  ppm for  $^{207}\text{Pb}/^{206}\text{Pb}$ ,  $^{208}\text{Pb}/^{206}\text{Pb}$  and  $\sim 300$ – $700$  ppm for  $^{20x}\text{Pb}/^{204}\text{Pb}$  (Table 3). Given this discrepancy, it is most likely that the external 2sd reproducibility of the seawater Pb isotope data is limited by contamination of the

samples by blanks of both variable magnitude and isotope composition. This interpretation is supported by two observations. First, the Weddell seawater, which has the lowest Pb concentration and thus the smallest Pb sample sizes, generally features the largest 2sd uncertainties (Table 3). Second, the application of a blank correction did not improve the 2sd reproducibilities for any of the samples, regardless of whether the corrections used mean blank values or only blank data that were linked to a specific batch of samples. In addition, it is also conceivable that the between-run 2sd uncertainties of the samples (Table 3) are, at least in part, limited by minor isotope fractionations that occur during the column chemistry (Fig. 1).

### 3.5. GEOTRACES intercalibration samples GSI and GDI

Multiple Pb isotope and concentration measurements were also carried out for the two GEOTRACES intercomparison samples GSI and GDI (Table 4). For the Pb concentrations, GEOTRACES 'consensus values' were recently published, which are based on analyses of more than 10 independent laboratories [53]. The mean Pb concentrations determined for the samples in this study from analyses of five or six separate aliquots have  $\pm 1\text{sd}$  (external) reproducibilities that are similar to those obtained for the in-house seawater reference samples (Table 3), at about  $\pm 4$  to  $\pm 6\%$  (Table 4). The results are, furthermore, identical to the reference values within the quoted uncertainties (Table 4).

The Pb isotope data for GSI and GDI were obtained on 2–3 sample aliquots of 2 L each, with originally about 10–15 ng Pb (Table 4). Following chemical separation, about 5–10 ng Pb were available for isotopic analysis. As for the seawater results of Table 3, the GSI and GDI measurements achieved (within-run) 2se repeatabilities that are similar to those obtained for similar loads of pure SRM 981 Pb, at 30–60 ppm for  $^{207}\text{Pb}/^{206}\text{Pb}$ ,  $^{208}\text{Pb}/^{206}\text{Pb}$  and 150–200 ppm for  $^{20x}\text{Pb}/^{204}\text{Pb}$  (Table 4). In contrast, the external 2sd uncertainties, of  $\sim 650$ – $1500$  ppm for  $^{207}\text{Pb}/^{206}\text{Pb}$ ,  $^{208}\text{Pb}/^{206}\text{Pb}$  and  $\sim 500$ – $2200$  ppm for  $^{20x}\text{Pb}/^{204}\text{Pb}$ , are typically significantly larger (Table 4). Again, this is most likely due to small Pb blank contributions of variable magnitude and isotope compositions and, potentially, minor isotope fractionation during Pb purification. Despite of this, our results for the two samples compare favorably and are generally in agreement with the published reference results.

The reference Pb isotope data for the GEOTRACES samples were obtained at MIT (Massachusetts Institute of Technology) using MC-ICP-MS and at UCSC (University of California at Santa Cruz) by HR-ICP-MS [35]. These analyses did not apply a Pb double spike and were carried out using significantly smaller samples sizes (of about 0.25–0.5 L) compared to those utilized here.

For GSI, all Pb isotope ratios determined are identical to the MIT results within the 2sd uncertainties. There is also good agreement with the UCSC results for  $^{207}\text{Pb}/^{206}\text{Pb}$ ,  $^{208}\text{Pb}/^{206}\text{Pb}$  but the UCSC data are higher for  $^{20x}\text{Pb}/^{204}\text{Pb}$  (Table 4). The uncertainties of the UCSC data are only poorly characterized, however, as they are based on only two analyses of a single seawater aliquot. Our new isotopic data for GDI are in excellent agreement with the MIT and UCSC results for  $^{207}\text{Pb}/^{206}\text{Pb}$ ,  $^{208}\text{Pb}/^{206}\text{Pb}$  and in reasonable agreement, just within uncertainty, with the UCSC  $^{206}\text{Pb}/^{204}\text{Pb}$  and  $^{208}\text{Pb}/^{204}\text{Pb}$  ratios (Table 4). Hence, there are small but significant discrepancies for the remaining  $^{20x}\text{Pb}/^{204}\text{Pb}$  data with the reference values, whereby our ratios are slightly lower. There is, however, also only marginal agreement between the MIT and UCSC results for these Pb isotope ratios, which are difficult to determine due to the low natural abundance of  $^{204}\text{Pb}$ . This indicates that further analyses are needed to establish more reliable reference data for the  $^{20x}\text{Pb}/^{204}\text{Pb}$  ratios of the GEOTRACES intercalibration samples.



The particular difficulty of  $^{204}\text{Pb}$  measurements is also apparent in a comparison of the reproducibilities for the Pb isotope data obtained here and previously [35]. For the  $^{208}\text{Pb}/^{204}\text{Pb}$  ratios, the multiple MIT analyses reveal a  $\pm 2\text{sd}$  uncertainty of  $\sim 5000$ – $10,000$  ppm, whilst our data for GSI, GDI (Table 4) and the in-house test samples (Table 3) have uncertainties which are at least a factor of 5 better, at  $\sim 500$ – $2000$  ppm. For  $^{207}\text{Pb}/^{206}\text{Pb}$  and  $^{208}\text{Pb}/^{206}\text{Pb}$  the difference is less apparent, however, as the reproducibility of the MIT results varies between 500 and 2500 ppm, whilst the data of this study (Tables 3 and 4) typically have an uncertainty of about 500–1500 ppm.

### 3.6. Depth profile for Pb isotopes and concentrations in the eastern South Atlantic Ocean

Twelve seawater samples from a depth profile in the eastern part of the GEOTRACES GA10 section in the South Atlantic Ocean were analyzed (Fig. 2a and Table 5), to (i) demonstrate that our new methodology is suitable for routine acquisition of high precision seawater Pb isotope data and (ii) highlight the important insights, which can be gained from such results.

Lead concentrations are highest in the uppermost part of the water column with a surface ( $\sim 3$  m water depth) concentration of 17.7 pmol/kg, increasing to a relative maximum of 25.2 pmol/kg at 49 m and decreasing again to 22.4 pmol/kg at 397 m depth. From 400 m downwards, the Pb concentrations decrease, until they reach relatively constant and low values of 5–10 pmol/kg below 2000 m (Fig. 2a). A comparison with the dissolved Pb concentrations for a depth profile collected at the exact same location during the second expedition along the South Atlantic GA10 transect (cruise JC068; same station; Schlosser et al., pers. comm.) demonstrates excellent agreement for the entire water column. In contrast, data reported from IPY cruise MD166 (Boye et al. [36]) for the same location show significant deviations from our results, as the dissolved Pb concentrations are elevated by up to a factor of 2 and they define a pattern which is less smooth with depth.

Overall, our Pb concentrations for seawater from the southeast Atlantic Ocean, sampled in 2010, are significantly lower than the values of 29.5 pmol/kg and 42.2 pmol/kg that were reported for 2008 samples from the surface and 2000 m depth at the BATS station in the northwest Atlantic Ocean (Table 4). Lead concentrations in seawater have been strongly affected by anthropogenic Pb emissions over the past century. Such emissions were generally higher in the northern Hemisphere compared to southern regions but peaked in the 1970s. Since then, they have decreased by almost

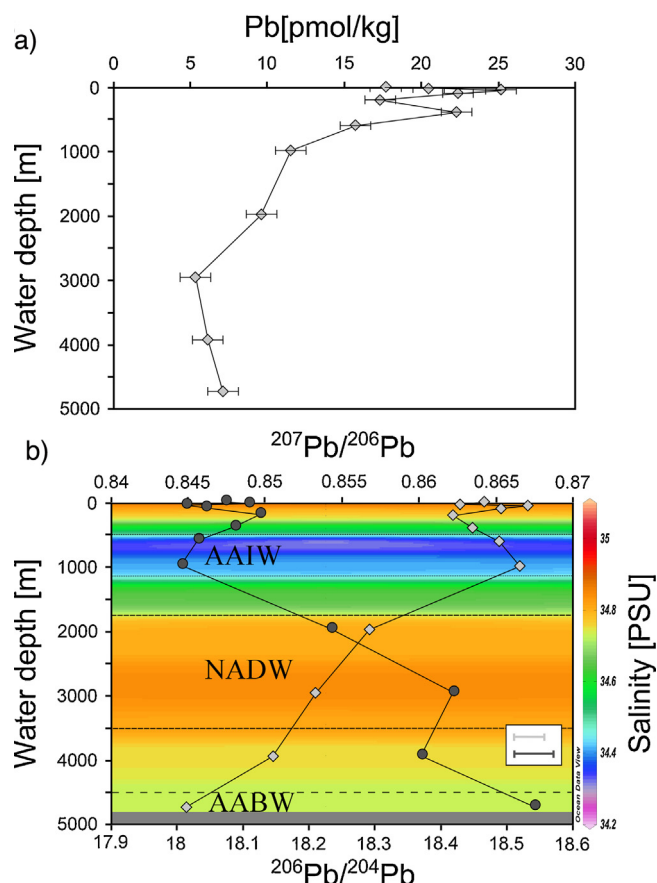


Fig. 2. Lead data for the seawater depth profile collected at station 3 (36.46°S, 13.39°E) of the GEOTRACES GA10 cruise. (A) Vertical distribution of Pb concentrations, with uncertainties as reported in Table 4 and (B) vertical distribution of  $^{207}\text{Pb}/^{206}\text{Pb}$  (grey diamonds) and  $^{206}\text{Pb}/^{204}\text{Pb}$  (dark grey dots) ratios, with uncertainties as reported in Table 4. The background colors from Ocean Data View [59] display the salinity of the water column during the time of sample collection [37].

a factor of 10 due to the phasing out of leaded gasoline, first in the US and then in Europe (e.g., Kelly et al. [16]). Consequently, northwest Atlantic surface waters now contain less anthropogenic Pb (and exhibit a different isotopic composition) than deeper North Atlantic waters, which were contaminated in the past [13,19]. A

Table 5

Lead isotope and concentration data for a seawater profile from the southeastern Atlantic Ocean (D357 station 3, GEOTRACES transect GA10; latitude: 36.46°S, longitude: 13.39°E; sampled in October 2010).

Sample	Depth (m)	[Pb] pmol/kg <sup>a</sup>	$\pm 1\text{sd}^b$	$^{206}\text{Pb}/^{204}\text{Pb}^c$	$^{207}\text{Pb}/^{204}\text{Pb}^c$	$^{208}\text{Pb}/^{204}\text{Pb}^c$	$^{207}\text{Pb}/^{206}\text{Pb}^c$	$^{208}\text{Pb}/^{206}\text{Pb}^c$
Fish 113	2–3	17.7	0.9	18.073	15.620	38.030	0.86428	2.1040
183	25	20.5	0.4	18.111	15.624	38.017	0.86266	2.0991
180	49	25.2	0.5	18.013	15.618	37.922	0.86707	2.1053
177	99	22.4	0.8	18.044	15.614	37.941	0.86533	2.1027
174	198	17.3	0.6	18.125	15.627	38.015	0.86221	2.0975
171	397	22.3	0.6	18.087	15.618	37.970	0.86350	2.0993
170	594	15.7	0.5	18.031	15.600	37.885	0.86518	2.1011
169	989	11.5	0.5	18.007	15.604	37.911	0.86655	2.1052
167	1975	9.6	0.4	18.234	15.623	38.159	0.85677	2.0927
166	2955	5.3	0.4	18.418	15.717	38.452	0.85331	2.0879
164	3931	6.1	0.4	18.370	15.625	38.266	0.85050	2.0830
163	4724	7.1	0.4	18.540	15.664	38.537	0.84492	2.0785

<sup>a</sup> Pb concentrations are corrected for a mean total blank of  $11.7 \pm 4.3$  pg.

<sup>b</sup> The uncertainties of the concentration data propagate both the (within-run) precision of the isotopic analyses and the uncertainty of the blank correction (see text).

<sup>c</sup> For the Pb isotopes, assumed external 2sd reproducibilities of  $\pm 1250$  ppm for  $^{208}\text{Pb}/^{204}\text{Pb}$  and of  $\pm 800$  ppm for  $^{207}\text{Pb}/^{206}\text{Pb}$ ,  $^{208}\text{Pb}/^{206}\text{Pb}$  are larger than the  $\pm 2\text{se}$  internal uncertainties in all cases. Based on this, appropriate 2sd uncertainties are  $\pm 0.023$  for  $^{206}\text{Pb}/^{204}\text{Pb}$ ,  $\pm 0.020$  for  $^{207}\text{Pb}/^{204}\text{Pb}$ ,  $\pm 0.047$  to  $0.048$  for  $^{208}\text{Pb}/^{204}\text{Pb}$ ,  $\pm 0.00068$  to  $0.00069$  for  $^{207}\text{Pb}/^{206}\text{Pb}$  and  $\pm 0.0017$  for  $^{208}\text{Pb}/^{206}\text{Pb}$ .

comparison of our (sub-) surface Pb concentrations (18–25 pmol/L) with data for eastern South Atlantic surface waters sampled in 1990 (with [Pb] = 11–29 pmol/kg at 21–32°S and 7–13°E; [47]) reveals similar results. This implies that there was no major change in the Pb supply to the southeast Atlantic Ocean between 1990 and 2010.

The  $^{207}\text{Pb}/^{206}\text{Pb}$  isotope ratios for our seawater profile from the South Atlantic exhibit the highest values in the subsurface and at mid depth (0.867 at 49 m and 989 m water depth) and slightly lower values at the surface and at 198 m ( $^{207}\text{Pb}/^{206}\text{Pb} \approx 0.862$ – $0.863$ ; Fig. 2b). Below  $\sim 1000$  m water depth,  $^{207}\text{Pb}/^{206}\text{Pb}$  decreases all the way to the bottom of the profile ( $^{207}\text{Pb}/^{206}\text{Pb} = 0.845$  at 4723 m water depth). These trends in  $^{207}\text{Pb}/^{206}\text{Pb}$  are mirrored by the  $^{206}\text{Pb}/^{204}\text{Pb}$  ratios, which are lowest at the subsurface ( $^{206}\text{Pb}/^{204}\text{Pb} = 18.01$ ; 49 m) and at intermediate depth ( $^{206}\text{Pb}/^{204}\text{Pb} = 18.01$ ; 989 m), and increase to  $^{206}\text{Pb}/^{204}\text{Pb} = 18.54$  at the bottom of the profile (Fig. 2b). The correlation between the seawater  $^{207}\text{Pb}/^{206}\text{Pb}$  and  $^{206}\text{Pb}/^{204}\text{Pb}$  ratios ( $r^2 = 0.97$ ) observed here is significantly improved compared to the results of previous studies [13,19,20,23,54]. We assign this improvement to the accurate and precise determination of the minor isotope  $^{204}\text{Pb}$  (and hence  $^{206}\text{Pb}/^{204}\text{Pb}$  ratios) with our new methodology, and surmise that previous claims of poor correlations may be due to analytical artifacts and should hence be assessed with care.

The major deep and intermediate water masses encountered at station 3 in the eastern South Atlantic are indicated by the salinity contouring in Fig. 2b. In brief, most of the water column is dominated by water masses sourced from high southern latitudes – cold and dense Antarctic bottom water (AABW) at  $>4500$  m depth, and fresh Antarctic intermediate water (AAIW) at  $\sim 500$ – $1100$  m – whilst saline, nutrient-poor North Atlantic Deep Water (NADW) is present at  $\sim 1700$ – $3500$  m depth (see Wyatt et al. [37] for further details on the transect hydrography). Since we are presenting the first Pb isotope depth profile for the eastern South Atlantic, there are no data available for direct comparison. However, our results confirm previously suggested differences [23] in the Pb isotope fingerprints of two main Southern Ocean water masses, AAIW ( $^{207}\text{Pb}/^{206}\text{Pb} = 0.865$ – $0.867$ ,  $^{206}\text{Pb}/^{204}\text{Pb} = 18.01$ – $18.03$ ;  $n = 2$ ) and AABW ( $^{207}\text{Pb}/^{206}\text{Pb} = 0.845$ ,  $^{206}\text{Pb}/^{204}\text{Pb} = 18.54$ ;  $n = 1$ ). These isotopic differences are a consequence of different water mass formation mechanisms and regions (e.g., Orsi et al. [55]), and hence different proportions of anthropogenic versus natural Pb, prior to ventilation into the deeper ocean. The Pb isotopic composition of NADW in the southeast Atlantic Ocean ( $^{207}\text{Pb}/^{206}\text{Pb} = 0.853$ – $0.857$ ,  $^{206}\text{Pb}/^{204}\text{Pb} = 18.42$ – $18.23$  at  $\sim 2000$ – $3000$  m water depth;  $n = 2$ ) appears distinct from NADW in the northwestern North Atlantic (BATS Station at 2000 m; Table 4), and values previously reported for the equatorial western Atlantic Ocean [23]. This points to older ventilation ages in the eastern basins of the Atlantic Ocean compared to the western basins (e.g., England [56]). Further interpretation of the results will, however, have to await the acquisition of Pb isotope and concentration data for additional profiles from the GEOTRACES GA10 transect.

#### 4. Conclusions

A new analytical procedure has been developed for Pb isotope analysis of seawater and associated Pb concentration measurements by isotope dilution. This involves Mg hydroxide co-precipitation and anion exchange chromatography for Pb pre-concentration and isotopic analysis by TIMS in conjunction with a  $^{207}\text{Pb}$ – $^{204}\text{Pb}$  double spike. Analyses of multiple aliquots of six seawater samples demonstrate typical reproducibilities ( $\pm 2\text{sd}$ ) of about 700–1500 ppm and 1000–2000 ppm for  $^{207}\text{Pb}/^{206}\text{Pb}$ ,  $^{208}\text{Pb}/^{206}\text{Pb}$  and  $^{206}\text{Pb}/^{204}\text{Pb}$ ,  $^{207}\text{Pb}/^{204}\text{Pb}$ ,  $^{208}\text{Pb}/^{204}\text{Pb}$ , respectively. With this

precision, the new data are superior to literature results that were obtained by plasma source mass spectrometry. In particular, they are at least a factor of five more precise for ratios involving the minor  $^{204}\text{Pb}$  isotope. Analyses of two GEOTRACES intercalibration samples from the Atlantic Ocean (GDI and GSI) display good agreement with recent results of two other laboratories.

Our methods were applied to samples from a seawater depth profile from the eastern South Atlantic Ocean at  $\sim 40^\circ\text{S}$ . For these samples, both Pb concentrations and isotope compositions show a smooth pattern with depth and no obvious outliers. Furthermore,  $^{206}\text{Pb}/^{204}\text{Pb}$  shows a clear correlation with  $^{207}\text{Pb}/^{206}\text{Pb}$ , underlining the improvement that was achieved for the challenging Pb isotope analyses, particularly of  $^{206}\text{Pb}/^{204}\text{Pb}$ . The depth profile results permit the identification and characterization of several key water masses, including AAIW, AABW and NADW. Considering that our profile is not located far from the formation regions of AAIW and AABW, the data provide the most precise Pb isotope characterization of these water masses published to date, but substantiation of the results by analyses of additional seawater samples from this region is needed.

#### Acknowledgements

We thank all of the MAGIC team for helping to keep spirits high, the mass spec running and the clean labs clean, and are particularly grateful for the vital support provided by Barry Coles and Katharina Kreissig. Ed Boyle volunteered helpful tips during method development, first suggesting the use of trace HF during column chemistry. The scientific party (principal scientist Gideon Henderson), technicians and crew of the R.R.S. Discovery on GEOTRACES cruise D357 are thanked for collection of the South Atlantic seawater profile. The supportive and helpful comments of two anonymous referees and swift editorial handling were also highly appreciated. Financial support for this study was provided by NERC consortium grant NE/H006095/1 to the UK GEOTRACES program and D. Weiss, T. van de Flierdt and M. Rehkämper at Imperial College.

#### References

- [1] S.W. Group, GEOTRACES – an international study of the global marine biogeochemical cycles of trace elements and their isotopes, *Chem. Erde – Geochem.* 67 (2007) 85–131.
- [2] T.J. Chow, M.S. Johnstone, Lead isotopes in gasoline and aerosols of Los Angeles basin, California, *Science* 147 (1965) 502–503, doi:http://dx.doi.org/10.1126/science.147.3657.502.
- [3] T.J. Chow, J.L. Earl, Lead isotopes in North American coals, *Science* 176 (1972) 510–511.
- [4] T.J. Chow, K.W. Bruland, K. Bertine, A. Soutar, M. Koide, E.D. Goldberg, Lead pollution: records in Southern California coastal sediments, *Science* 181 (1973) 551–552.
- [5] T.J. Chow, J.L. Earl, Lead aerosols in the atmosphere: increasing concentrations, *Science* 169 (1970) 577–580.
- [6] A.R. Flegal, C.C. Patterson, Vertical concentration profiles of lead in the Central Pacific at 15°N and 20°S, *Earth Planet. Sci. Lett.* 64 (1983) 19–32, doi:http://dx.doi.org/10.1016/0012-821X(83)90049-3.
- [7] B.K. Schaule, C.C. Patterson, Perturbations of the natural lead depth profile in the sargasso sea by industrial lead, in: C.S. Wong, E. Boyle, K. Bruland, J.D. Burton, E. Goldberg (Eds.), *Trace Metals Sea Water*, Springer, US, 1983, pp. 487–503, doi:http://dx.doi.org/10.1007/978-1-4757-6864-0\_29.
- [8] B.K. Schaule, C.C. Patterson, Lead concentrations in the northeast Pacific: evidence for global anthropogenic perturbations, *Earth Planet. Sci. Lett.* 54 (1981) 97–116, doi:http://dx.doi.org/10.1016/0012-821X(81)90072-8.
- [9] C.C. Patterson, D. Settle, B. Glover, Analysis of lead in polluted coastal seawater, *Mar. Chem.* 4 (1976) 305–319.
- [10] A.R. Flegal, T.F. Duda, S. Niemyer, High gradients of lead isotopic composition in north-east Pacific upwelling filaments, *Nature* 339 (1989) 458–460, doi:http://dx.doi.org/10.1038/339458a0.
- [11] A.R. Flegal, B.K. Schaule, C.C. Patterson, Stable isotopic ratios of lead in surface waters of the Central Pacific, *Mar. Chem.* 14 (1984) 281–287, doi:http://dx.doi.org/10.1016/0304-4203(84)90048-3.
- [12] G.T. Shen, E.A. Boyle, Thermocline ventilation of anthropogenic lead in the western North Atlantic, *J. Geophys. Res. Oceans* 93 (1988) 15715–15732, doi:http://dx.doi.org/10.1029/JC093iC12p15715.

- [13] A.J. Véron, T.M. Church, C. Patterson, A.R. Flegal, Use of stable lead isotopes to characterize the sources of anthropogenic lead in North Atlantic surface waters, *Geochim. Cosmochim. Acta* 58 (1994) 3199–3206, doi:[http://dx.doi.org/10.1016/0016-7037\(94\)90047-7](http://dx.doi.org/10.1016/0016-7037(94)90047-7).
- [14] D. Weiss, E.A. Boyle, V. Chavagnac, M. Herwegh, J. Wu, Determination of lead isotope ratios in seawater by quadrupole inductively coupled plasma mass spectrometry after Mg(OH)<sub>2</sub> co-precipitation, *Spectrochim. Acta, Part B At. Spectrosc.* 55 (2000) 363–374.
- [15] M.K. Reuer, E.A. Boyle, B.C. Grant, Lead isotope analysis of marine carbonates and seawater by multiple collector ICP-MS, *Chem. Geol.* 200 (2003) 137–153, doi:[http://dx.doi.org/10.1016/S0009-2541\(03\)00186-4](http://dx.doi.org/10.1016/S0009-2541(03)00186-4).
- [16] A.E. Kelly, M.K. Reuer, N.F. Goodkin, E.A. Boyle, Lead concentrations and isotopes in corals and water near Bermuda, 1780–2000, *Earth Planet. Sci. Lett.* 283 (2009) 93–100.
- [17] A. Véron, P. Flament, M.L. Bertho, L. Alleman, R. Flegal, B. Hamelin, Isotopic evidence of pollutant lead sources in Northwestern France, *Atmos. Environ.* 33 (1999) 3377–3388, doi:[http://dx.doi.org/10.1016/S1352-2310\(98\)00376-8](http://dx.doi.org/10.1016/S1352-2310(98)00376-8).
- [18] D. Weiss, E.A. Boyle, J. Wu, V. Chavagnac, A. Michel, M.K. Reuer, Spatial and temporal evolution of lead isotope ratios in the North Atlantic Ocean between 1981 and 1989, *J. Geophys. Res. Oceans* 108 (2003) 3306, doi:<http://dx.doi.org/10.1029/2000JC000762>.
- [19] B. Hamelin, J.L. Ferrand, L. Alleman, E. Nicolas, A.J. Véron, Isotopic evidence of pollutant lead transport from North America to the subtropical North Atlantic gyre, *Geochim. Cosmochim. Acta* 61 (1997) 4423–4428, doi:[http://dx.doi.org/10.1016/S0016-7037\(97\)00242-1](http://dx.doi.org/10.1016/S0016-7037(97)00242-1).
- [20] A.J. Véron, T.M. Church, I. Rivera-Duarte, A.R. Flegal, Stable lead isotopic ratios trace thermohaline circulation in the subarctic North Atlantic, *Deep Sea Res. Part II Top. Stud. Oceanogr.* 46 (1999) 919–935.
- [21] F. von Blanckenburg, H. Igel, Lateral mixing and advection of reactive isotope tracers in ocean basins: observations and mechanisms, *Earth Planet. Sci. Lett.* 169 (1999) 113–128.
- [22] M.K. Reuer, D.J. Weiss, Anthropogenic lead dynamics in the terrestrial and marine environment, *Philos. Trans. R. Soc. Lond. Ser. Math. Phys. Eng. Sci.* 360 (2002) 2889–2904, doi:<http://dx.doi.org/10.1098/rsta.2002.1095>.
- [23] L.Y. Alleman, T.M. Church, P. Ganguli, A.J. Véron, B. Hamelin, A.R. Flegal, Role of oceanic circulation on contaminant lead distribution in the South Atlantic, *Deep Sea Res. Part II Top. Stud. Oceanogr.* 48 (2001) 2855–2876.
- [24] T. Hirata, Lead isotopic analyses of NIST standard reference materials using multiple collector inductively coupled plasma mass spectrometry coupled with a modified external correction method for mass discrimination effect, *Analyst* 121 (1996) 1407–1411.
- [25] F.W.E. Strelow, Distribution coefficients and anion exchange behavior of some elements in hydrobromic-nitric acid mixtures, *Anal. Chem.* 50 (1978) 1359–1361, doi:<http://dx.doi.org/10.1021/ac50031a041>.
- [26] G.W. Lugmair, S.J.G. Galer, Age and isotopic relationships among the angrites Lewis Cliff 86,010 and Angra dos Reis, *Geochim. Cosmochim. Acta* 56 (1992) 1673–1694.
- [27] B. Hamelin, G. Manhès, F. Albarède, C.J. Allègre, Precise lead isotope measurements by the double spike technique: a reconsideration, *Geochim. Cosmochim. Acta* 49 (1985) 173–182, doi:[http://dx.doi.org/10.1016/0016-7037\(85\)90202-9](http://dx.doi.org/10.1016/0016-7037(85)90202-9).
- [28] S.J.G. Galer, Optimal double and triple spiking for high precision lead isotopic measurement, *Chem. Geol.* 157 (1999) 255–274.
- [29] J. Baker, D. Peate, T. Waight, C. Meyzen, Pb isotopic analysis of standards and samples using a <sup>207</sup>Pb–<sup>204</sup>Pb double spike and thallium to correct for mass bias with a double-focusing MC-ICP-MS, *Chem. Geol.* 211 (2004) 275–303.
- [30] N.H. Gale, A solution in closed form for lead isotopic analysis using a double spike, *Chem. Geol.* 6 (1970) 305–310.
- [31] M.F. Thirlwall, Inter-laboratory and other errors in Pb isotope analyses investigated using a <sup>207</sup>Pb–<sup>204</sup>Pb double spike, *Chem. Geol.* 163 (2000) 299–322.
- [32] M.F. Thirlwall, Multicollector ICP-MS analysis of Pb isotopes using a <sup>207</sup>Pb–<sup>204</sup>Pb double spike demonstrates up to 400 ppm/amu systematic errors in TI-normalization, *Chem. Geol.* 184 (2002) 255–279.
- [33] J.D. Woodhead, F. Volker, M.T. McCulloch, Routine lead isotope determinations using a lead-207-lead-204 double spike: a long-term assessment of analytical precision and accuracy, *Analyst* 120 (1995) 35–39.
- [34] J.D. Woodhead, J.M. Hergt, Application of the 'double spike' technique to Pb-isotope geochronology, *Chem. Geol.* 138 (1997) 311–321.
- [35] E.A. Boyle, S. John, W. Abouchami, J.F. Adkins, Y. Echegoyen-Sanz, M. Ellwood, et al., GEOTRACES IC1 (BATS) contamination-prone trace element isotopes Cd, Fe, Pb, Zn, Cu, and Mo intercalibration, *Limnol. Oceanogr. Methods* 10 (2012) 653–665, doi:<http://dx.doi.org/10.4319/lom.2012.10.653>.
- [36] M. Boye, B.D. Wake, P. Lopez Garcia, J. Bown, A.R. Baker, E.P. Achterberg, Distributions of dissolved trace metals (Cd, Cu, Mn, Pb, Ag) in the southeastern Atlantic and the Southern Ocean, *Biogeosciences* 9 (2012) 3231–3246, doi:<http://dx.doi.org/10.5194/bg-9-3231-2012>.
- [37] N.J. Wyatt, A. Milne, A.P. Woodward, T.J. Browning, H.A. Bouman, et al., Biogeochemical cycling of dissolved zinc along the GEOTRACES South Atlantic transect GA10 at 40°S, *Glob. Biogeochem. Cycles* 28 (2014) 44–56, doi:<http://dx.doi.org/10.1002/2013GB004637>.
- [38] J.F. Rudge, B.C. Reynolds, B. Bourdon, The double spike toolbox, *Chem. Geol.* 265 (2009) 420–431.
- [39] W.M. White, F. Albarède, P. Télouk, High-precision analysis of Pb isotope ratios by multi-collector ICP-MS, *Chem. Geol.* 167 (2000) 257–270.
- [40] M. Rehkämper, A.N. Halliday, Accuracy and long-term reproducibility of lead isotopic measurements by multiple-collector inductively coupled plasma mass spectrometry using an external method for correction of mass discrimination, *Int. J. Mass Spectrom.* 181 (1998) 123–133.
- [41] M.H. Dodson, A theoretical study of the use of internal standards for precise isotopic analysis by the surface ionization technique: part 1 – general first-order algebraic solutions, *J. Sci. Instrum.* 40 (1963) 289–295, doi:<http://dx.doi.org/10.1088/0950-7671/40/6/307>.
- [42] J. Wu, E.A. Boyle, Lead in the western North Atlantic Ocean: completed response to leaded gasoline phaseout, *Geochim. Cosmochim. Acta* 61 (1997) 3279–3283.
- [43] P.M. Nicolaysen, E. Steinnes, T.E. Sjobakk, Pre-concentration of selected trace elements from seawater by co-precipitation on Mg(OH)<sub>2</sub>, *J. Phys. (IV Fr.)* 107 (2003) 945–948.
- [44] J. Wu, E.A. Boyle, Low blank preconcentration technique for the determination of lead copper, and cadmium in small-volume seawater samples by isotope dilution ICPMS, *Anal. Chem.* 69 (1997) 2464–2470.
- [45] G.F. de Souza, B.C. Reynolds, J. Rickli, M. Frank, M.A. Saito, L.J.A. Gerringa, et al., Southern Ocean control of silicon stable isotope distribution in the deep Atlantic Ocean: silicon isotopes in the deep Atlantic, *Glob. Biogeochem. Cycles* 26 (2012) 1944–19224, doi:<http://dx.doi.org/10.1029/2011GB004141>.
- [46] Y. Nozaki, K.K. Turekian, K. Von Damm, <sup>210</sup>Pb in GEOSECS water profiles from the North Pacific, *Earth Planet. Sci. Lett.* 49 (1980) 393–400.
- [47] W.I. Manton, Separation of Pb from young zircons by single-bead ion exchange, *Chem. Geol. Isot. Geosci. Sect.* 73 (1988) 147–152.
- [48] L.I. Guseva, A study of ion-exchange behavior of Pb in dilute HBr solutions, aimed to evaluate the possibility of on-line isolation of element 114 <sup>228</sup>Ra–<sup>212</sup>Pb generator, *Radiochemistry* 49 (2007) 92–96, doi:<http://dx.doi.org/10.1134/S106636220701016X>.
- [49] B.S. Kamber, A.H. Gladu, Comparison of Pb purification by anion-exchange resin methods and assessment of long-term reproducibility of Th/U/Pb ratio measurements by quadrupole ICP-MS, *Geostand. Geoanal. Res.* 33 (2009) 169–181, doi:<http://dx.doi.org/10.1111/j.1751-908X.2009.00911.x>.
- [50] H. Gerstenberger, G. Haase, A highly effective emitter substance for mass spectrometric Pb isotope ratio determinations, *Chem. Geol.* 136 (1997) 309–312.
- [51] R. Doucelance, G. Manhès, Reevaluation of precise lead isotope measurements by thermal ionization mass spectrometry: comparison with determinations by plasma source mass spectrometry, *Chem. Geol.* 176 (2001) 361–377.
- [52] J. Blichert-Toft, B. Zanda, D.S. Ebel, F. Albarède, The solar system primordial lead, *Earth Planet. Sci. Lett.* 300 (2010) 152–163.
- [53] The GEOTRACES Standards and Intercalibration Committee, *Consensus Values for the GEOTRACES 2008*, (2013).<http://www.geotraces.org/science/intercalibration/322-standards-and-reference-materials>.
- [54] L.Y. Alleman, T.M. Church, A.J. Véron, G. Kim, B. Hamelin, A.R. Flegal, Isotopic evidence of contaminant lead in the South Atlantic troposphere and surface waters, *Deep Sea Res. Part II Top. Stud. Oceanogr.* 48 (2001) 2811–2827.
- [55] A.H. Orsi, G.C. Johnson, J.L. Bullister, Circulation, mixing, and production of Antarctic bottom water, *Prog. Oceanogr.* 43 (1999) 55–109, doi:[http://dx.doi.org/10.1016/S0079-6611\(99\)00004-X](http://dx.doi.org/10.1016/S0079-6611(99)00004-X).
- [56] M.H. England, The age of water and ventilation timescales in a global ocean model, *J. Phys. Oceanogr.* 25 (1995) 2756–2777.
- [57] S.J.G. Galer, W. Abouchami, Practical application of lead triple spiking for correction of instrumental mass discrimination, *Miner. Mag.* 62A (1998) 491–492, doi:<http://dx.doi.org/10.1180/minmag.1998.62A.1.260>.
- [58] W. Todt, R.A. Cliff, A. Hanser, A.W. Hofmann, Evaluation of a <sup>202</sup>Pb–<sup>205</sup>Pb double spike for high – precision lead isotope analysis, in: A. Basu, S. Hart (Eds.), *Geophysical Monographs Series*, American Geophysical Union, Washington, D.C., 1996, pp. 429–437.
- [59] R. Schlitzer, *Ocean Data View*, (2002) <http://www.awi-bremerhaven.de/GEO/ODV>.